3-2009

Factors Influencing Contrast Resolution of Cone Beam CT Using the CB MercuRay

Roger M. Anderson

LOMA LINDA UNIVERSITY
School of Dentistry
in conjunction with the
Faculty of Graduate Studies

Factors Influencing Contrast Resolution of Cone Beam CT Using the CB MercuRay

by

Roger M. Anderson

This thesis is submitted in partial satisfaction
of the requirements for the degree of
Master of Science in Periodontics

March 2009

Each person whose signature appears below certifies that this thesis in his/her opinion is adequate, in scope and quality, as a thesis for the degree Master of Science.

____, Chairperson
Jeffrey Henkin, Associate Professor and Program Director of Periodontics,

____
Bernard Gantes, Adjunct Associate Professor of Periodontics

____
Max Crigger, Professor of Periodontics

____
Joseph M. Caruso, Associate Professor and Chair of the Department of Orthodontics and Dentofacial Orthopedics

____
Yoon Jeong Kim, Assistant Professor of Periodontics

ACKNOWLEDGEMENTS

I would like to express my appreciation to my guidance committee, Dr. Jeffrey Henkin, Dr. Bernard Gantes, Dr. Max Crigger, Dr. Joseph M. Caruso, and Dr. Yoon Jeong Kim. Additional thanks to Dr. Matt Riggs for statistical analysis as well as Dr. Eloy Shultz, Dr. Hyoung Jin Park, and Don Farley for their guidance. I am also grateful to Rite-Scan of Seal Beach which has donated usage of the CB MercuRay and technical support.

CONTENTS

TABLES

FIGURES

Figure Page

ABSTRACT

Factors Influencing Contrast Resolution of Cone Beam CT Using the CB MercuRay

by

Roger Anderson

Master of Science, Graduate Program in Periodontics
Loma Linda University, March 2009
Dr. Jeffrey Henkin, Chairperson

Introduction: Cone Beam Computed Tomography (CBCT) has an application in all dental specialties. CBCT is an aid in implant dentistry to evaluate anatomical landmarks in both quality and quantity. Hounsfield Unit (HU) values represent a grayscale that is standardized on CT machines relative to the density of water and air. It has been reported that the HU value represents an actual value of the bone density. However, recent studies at Loma Linda University have suggested that HU values retrieved using CBCT machines may be altered by various factors.

Purpose: The aim of this study is to evaluate the specific dosage factors (field of view, kVp, and mA) that influence the contrast resolution of images as measured by HU that are acquired from a phantom scanned with the CB MercuRay device.

Materials and Methods: A phantom was fabricated with 11 hydroxyapatite cylindrical disks with increasing mineral densities. Values ranged from a minimum of 0 mg/cm^3 up to a maximum of 1000 mg/cm^3. Scans with all available fields of View (FOV), kVp, and mA were stored and read with image viewing software. The variation of HU values with various adjustable settings was evaluated.

Results: HU values recorded varied significantly when changing adjustable settings. When changing among FOV and kVp, the HU were different statistically with ANOVA at $p \leq 0.001$. With further analysis it was found that each FOV was statistically different from each other with Bonferroni-corrected Post Hoc test at $p \leq 0.05$. The most variation in HU values was found with the 6 inch FOV. No statistically significant difference in HU values was found with changing the mA.

Conclusions: The HU values vary significantly by the FOV and kVp settings with CB MercuRay CBCT. Reducing amperage from 15 mA to 2 mA had very little effect on the HU values.

KEY WORDS: Cone Beam Computed Tomography, CB MercuRay, bone density, hydroxyapatite phantom, Hounsfield Unit, dental implant, scan field of view, dosage settings.

CHAPTER ONE

INTRODUCTION

Implant failures in poor bone quality[1] have led to studies that evaluate bone density.[2, 3] Lekholm and Zarb proposed a subjective classification of bone density based radiographs and the force felt by the surgeon's hands while placing implants. [4] Misch developed a classification of bone density that included guidelines for implant treatment planning. [5] Johansson and Strid showed the benefits of instant feedback with hand pieces with a torque value reading that may be correlated to implant success. [6]

The Hounsfield Unit (HU) obtained from evaluating a scan is another diagnostic tool that may aid in implant placement. HU values are a grayscale that is standardized on Computed Tomography (CT) machines relative to the density of water and air. Hounsfield suggested that image quality is similar to conventional radiography in that it still relies on the photons traveling from the source (cone) to the target (film) to create an image. [7] Photons that are absorbed or scattered result in a lighter image where the photons that reach the film produce darker images. The intensity of the photons reaching the film is described in kVp and the volume as mA. The kVp and mA must be adjusted to gain the maximum amount of contrast resolution to differentiate tissues based on their grayscale.

Norton and Gamble used CT to relate HU values[8] with the subjective bone evaluation of Lekholm and Zarb. [4] A number of studies have been done to evaluate bone density using CT. [9-12] The information gained from imaging with CT is meaningful, but the dose of radiation may limit its usefulness in dentistry.

The current solution to concerns of radiation dosage has been met with the Cone Beam Computed Tomography (CBCT). CBCT has found uses in multiple fields of dentistry. [13-16] CBCT units are highly accurate when measuring linear distances in the Field of View (FOV) [17-21] and compares favorably with CT. [22, 23]

Recent studies show that CBCT scans of bone density measured in HU values, are altered by FOV, kVp, and mA . [24-26] Araki and colleagues[25] found that by changing the mA and exposure mode, there would be more noise that effectively changes the relative CT number. Their experiment used a single density water phantom to demonstrate that there is variation in HU values with a change in tube current or FOV. Park[24] showed significant variations in HU values with the automated Smart Beam control of current and exposure mode in the Newtom 3G CBCT. The same group[26] also showed significant variations in HU when changing the FOV in the ICAT CBCT. The variations found upon assessing HU from CBCT devices make clinical judgments based on these values questionable.

Aiming at lowering patient exposure to radiation, Hitachi has modified the existing CB MercuRay hardware and software to allow a lower dosage of 2 mA. The advantage of this low dose may allow routine CBCTs for procedures previously limited to conventional radiographs. It is important to evaluate the quality of this low dosage radiograph and to determine if this upgrade has affected HU values reproducibility. Knowing the factors affecting HU value assessment will become an essential step in the future clinical application of relating implant success to bone density. The aim of this study is to evaluate three adjustable settings (FOV, kVp, and mA) that influence the contrast resolution of images acquired from a phantom scanned with the CB MercuRay.

CHAPTER TWO

MATERIALS AND METHODS

Phantom

The phantom was custom built utilizing 11 hydroxyapatite cylindrical disks (CIRS, USA) with different mineral densities starting at 25 mg/cm^3 then to 100 mg/cm^3 then increasing in 100 mg/cm^3 increments to 1000 mg/cm^3. Each disk is 2 cm in diameter and 1 cm in height. The eleven disks are stacked in a single column in consecutive descending order of known mineral densities. The column is secured in an airtight polyethylene container filled with vacuumed distilled water (Figure 1).

CBCT Machine

The CB MercuRay (12 bit; Hitachi Medical Corporation, Twinsburg Ohio) was utilized.

Acquisition of CBCT Images

The CB MercuRay was calibrated to air immediately before scanning the phantom. The phantom was placed in a position so that the radiation was perpendicular to the long axis of HA column and would capture the entire column of disks in a single scan. All combinations of the following settings were utilized in scanning the phantom: FOV of 6, 9, and 12 inch, kVp of 100 and 120, and mA of 2 and 15 (Table 1). Standard scanning procedures were used.

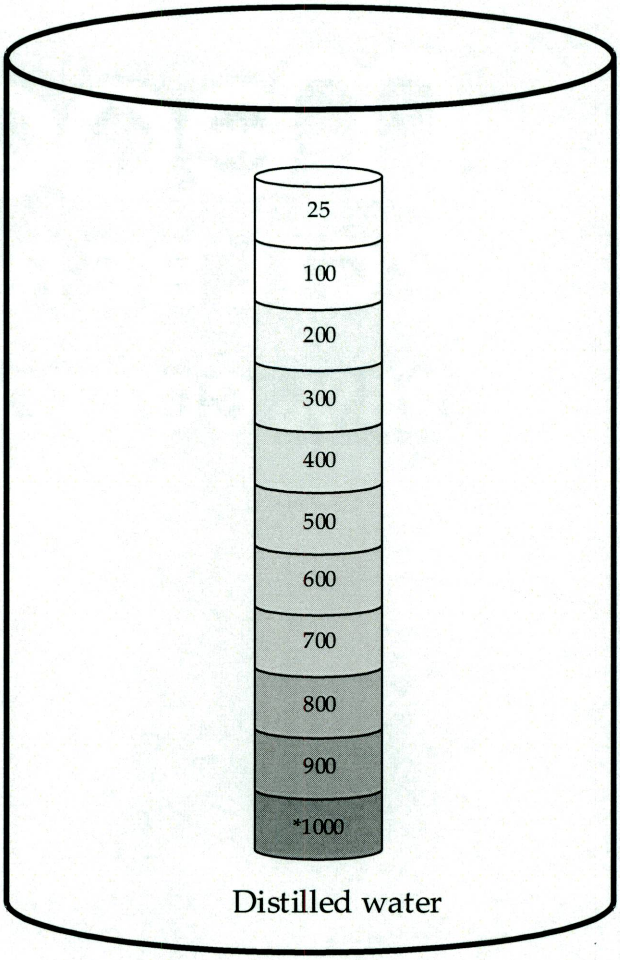

*Density of HA; mg/cm³

Figure 1. Illustration of the phantom consisting of stacked HA disks in consecutive order of known density.

Table 1. CB MercuRay adjustable settings.

FOV	6 inch				9 inch				12 inch			
mA	2		15		2		15		2		15	
kVp	100	120	100	120	100	120	100	120	100	120	100	120

Mineral Density Measurements

Eleven images from each scan were reviewed on the DICOM image viewer (Vworks, version 4.0 Cybermed Inc, Seoul, Korea). A circular Region of Interest (ROI) was defined at the center of each disk on the DICOM image in an effort to limit the area of analysis within a 3 mm boundary. The Phantom is presented in both the vertical and horizontal plane to illustrate the location of the ROI (Figure 2, 3). The HU values of these ROIs defined on scan images were saved as JPEG format.

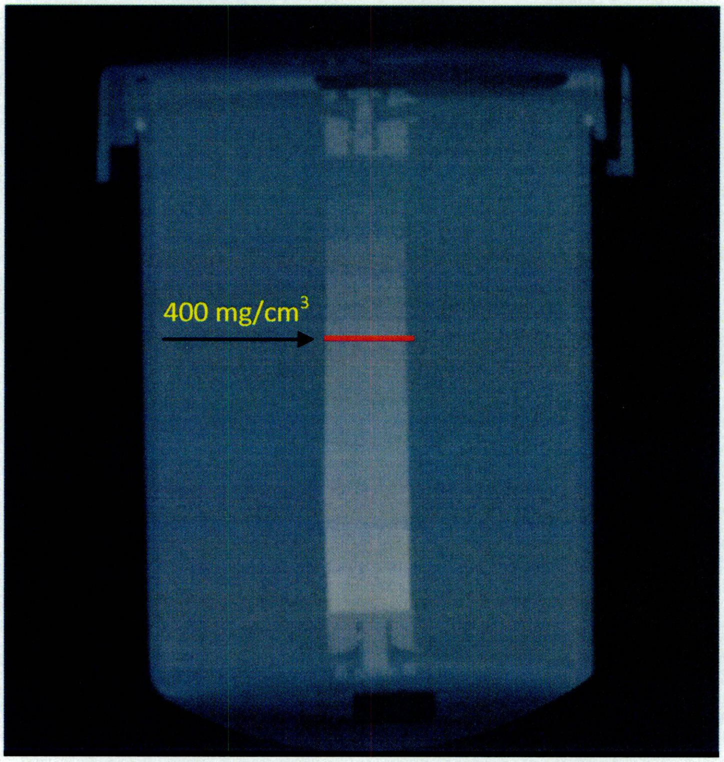

Figure 2. Vertical cross section of the phantom with region of interest at the 5th disk from the top correlating to the 400 mg/cm^3 HA disk.

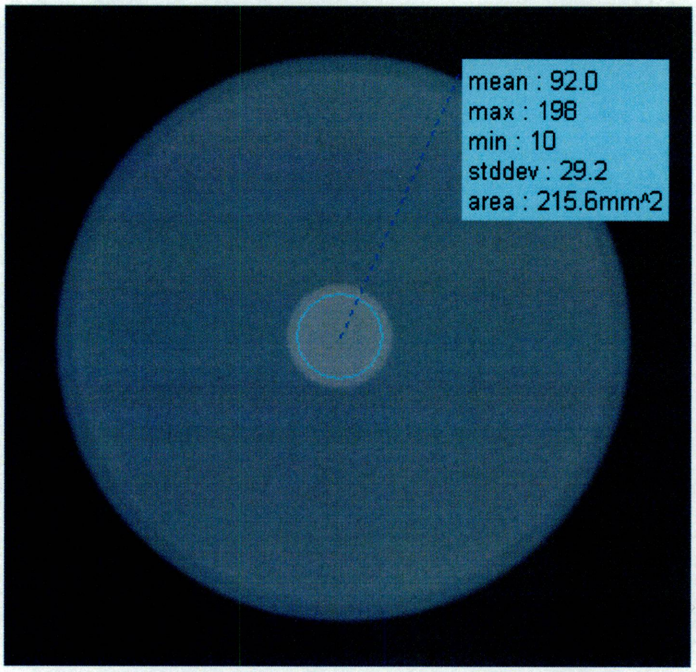

Figure 3. Horizontal cross section of the region of interest outlined on the 400 mg/cm^3 disk shown in Figure 2.

Data Analysis

All eleven disk scans were obtained at once for each FOV. Comparisons of HA mineral densities and measured HU values among the three different FOV, various kVp settings, and mA settings were performed using ANOVA with $p<0.001$. Additionally, comparisons of the HA mineral densities and corresponding HU values among the three different FOVs were compared with the Bonferroni Corrected Post Hoc test with $p<0.05$.

CHAPTER THREE

RESULTS

The 25 mg/cm^3 disk was difficult to differentiate from water resulting in limited data acquisition. Tables 2 through 5 show the overall data retrieved with the various settings. All recorded HU values are less than the known corresponding HA disk densities.

Table 2. HU values retrieved at 120 kVp and 15 mA with the 6, 9, and 12 inch scans.

HA (mg/cm^3)	120 kVp / 15 mA		
	6 inch	9 inch	12 inch
1000	692	746	453
900	530	631	380
800	445	534	316
700	428	465	267
600	405	400	211
500	343	325	153
400	225	242	92
300	65	152	19
200	-99	60	-57
100	-250	-39	-137
25	-322	-160	-214

Table 3. HU values retrieved at 100 kVp and 15 mA with the 6, 9, and 12 inch scans.

HA (mg/cm^3)	100 kVp / 15 mA		
	6 inch	9 inch	12 inch
1000	836	870	561
900	654	743	484
800	559	635	411
700	534	567	356
600	506	494	295
500	432	408	233
400	297	318	164
300	130	216	80
200	-50	108	-4
100	-220	-5	-93
25	-300	-138	-182

Table 4. HU values retrieved at 120 kVp and 2 mA with the 6, 9, and 12 inch scans.

HA (mg/cm^3)	120 kVp / 2 mA		
	6 inch	9 inch	12 inch
1000	713	754	480
900	550	637	413
800	468	544	350
700	458	483	306
600	429	415	253
500	364	338	193
400	240	255	125
300	75	167	53
200	-91	68	-22
100	-238	-33	-108
25	-301	-162	-191

Table 5. HU values retrieved at 100 kVp and 2 mA with the 6, 9, and 12 inch scans.

HA (mg/cm^3)	100 kVp / 2 mA		
	6 inch	9 inch	12 inch
1000	770	787	505
900	604	669	437
800	523	572	374
700	506	511	327
600	478	439	276
500	406	360	215
400	274	277	144
300	105	186	69
200	-70	84	-10
100	-237	-19	-97
25	-322	-150	-180

Figures 4-6 represent graphic regression displays of the datum for 6, 9 and 12 inch FOV across all measures of available settings. Figure 4A is an example showing the 6 inch FOV displaying a more pronounced S curve located generally between the values recorded for the 9 inch and 12 inch FOV. The S curve morphology is retained when the data is corrected to zero on x-y axis, but the relationship relative to the FOV is changed. The magnitude of differences between FOVs for 6 inch is 288 HU, for 9 inch 240 HU, and for 12 inch 496 HU. Each FOV is statistically significant from each other using an ANOVA test at $p<0.001$, and Bonferroni Corrected Post Hoc test at $p<0.05$. The Bonferonni Corrected Post Hoc test also shows that the 9 inch FOV is statistically different compared to the 6 and 12 inch FOV. The significant differences in the field of view were noted at all of the available kVp and mA settings.

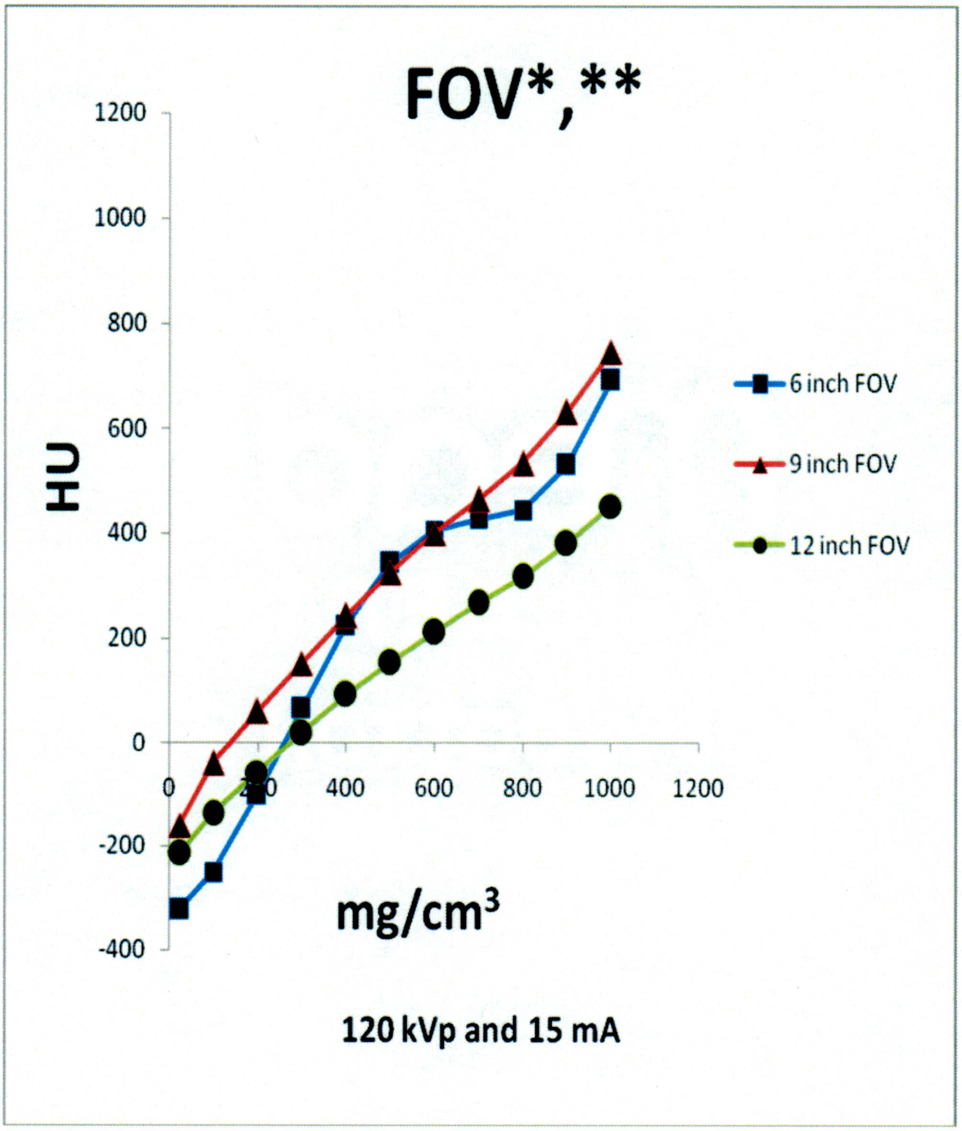

Figure 4. Plot of HU values of the three FOVs at 120 kVp and 15 mA. *ANOVA $p<0.001$, **Bonferroni Corrected Post Hoc $p<0.05$.

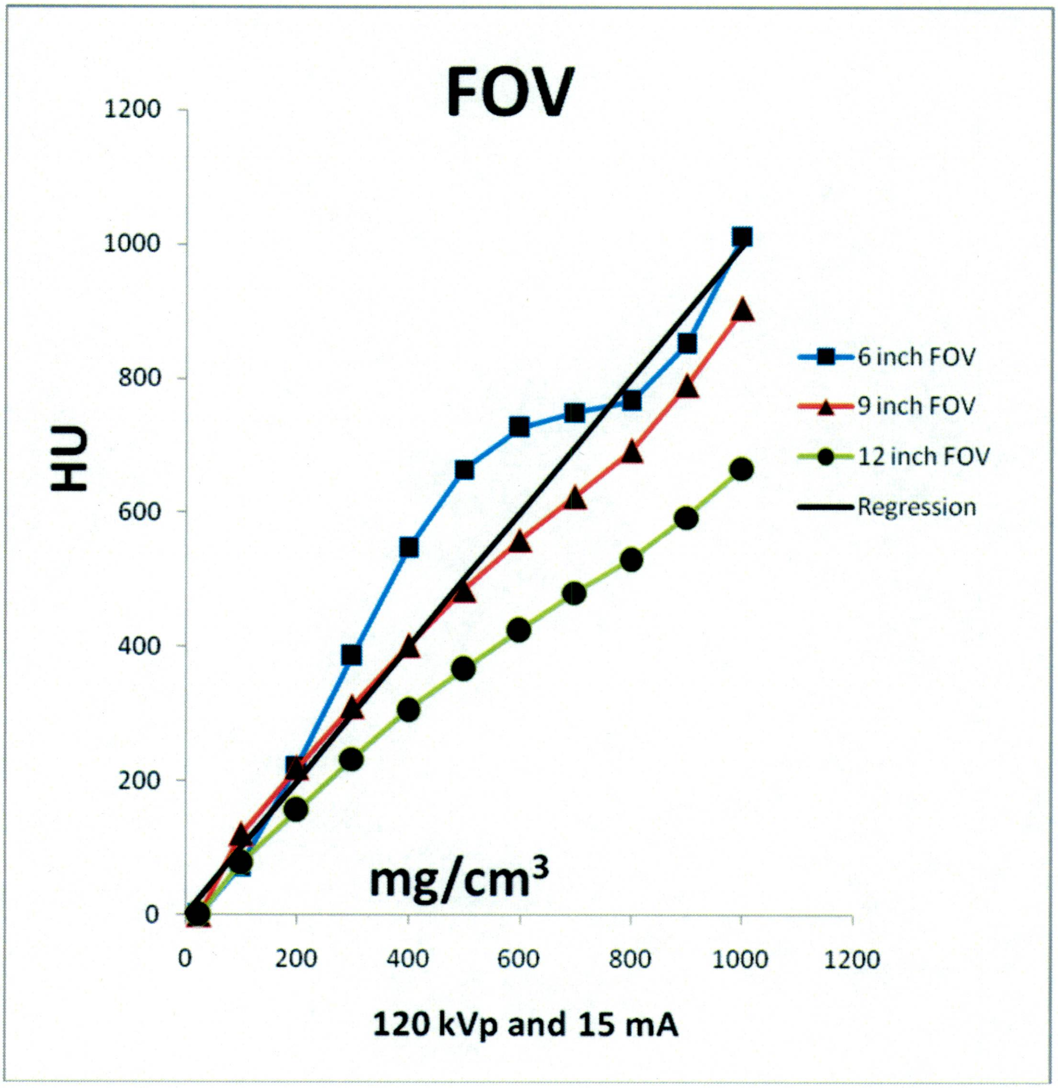

Figure 5. Plot of adjusted HU values to 0 baseline of the three FOVs at 120 kVp and 15 mA compared to a corrected regression line.

Changing kVp from 100 to 120 produces statistically significant differences using an ANOVA test at $p<0.001$, however, the magnitude of the largest difference found amounted to 128 HU. The significant difference in HU value measurements relative to kVp setting can be seen graphically at the 15 mA setting, but minimally at the 2 mA setting. (Figures 5-10)

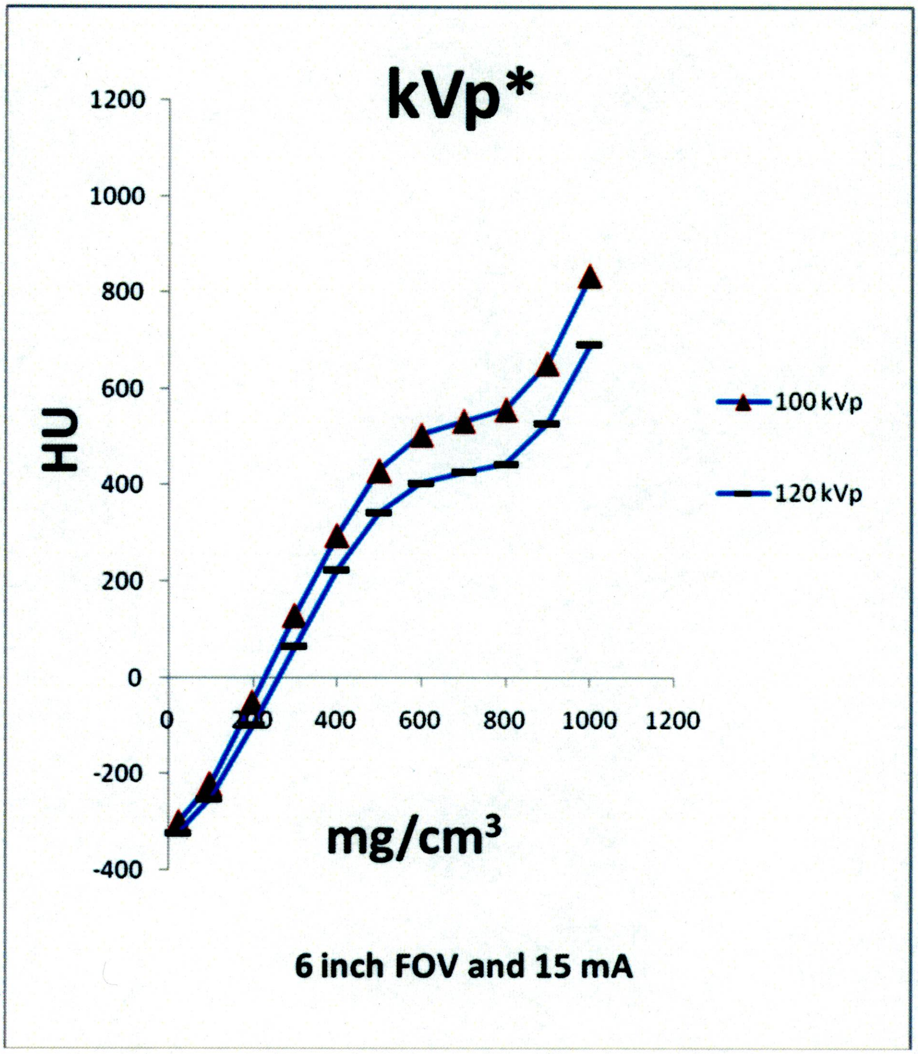

Figure 6. Plotted HU values comparing kVp at the 6 inch FOV and 15 mA.
*ANOVA $p<0.001$

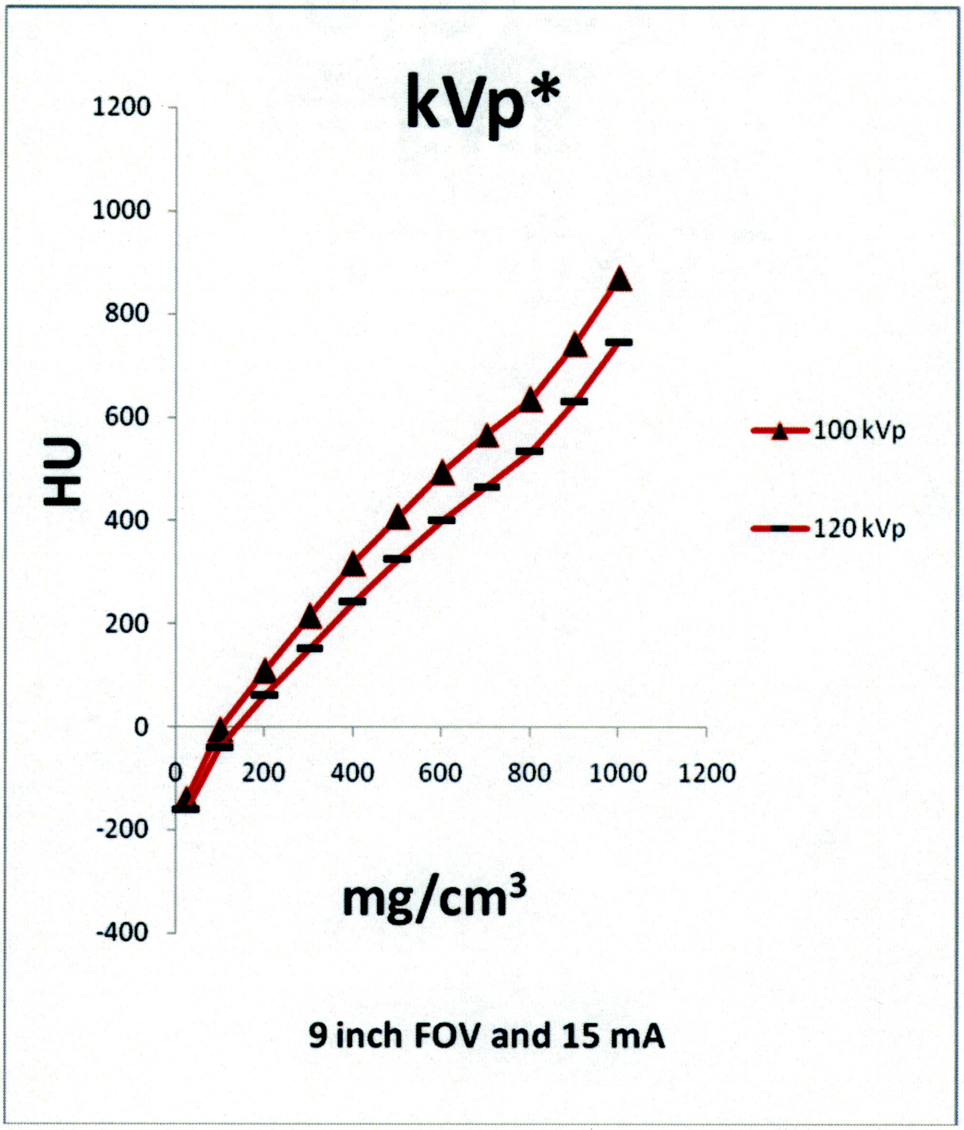

Figure 7. Plotted HU values comparing kVp at the 9 inch FOV and 15 mA.
*ANOVA $p<0.001$

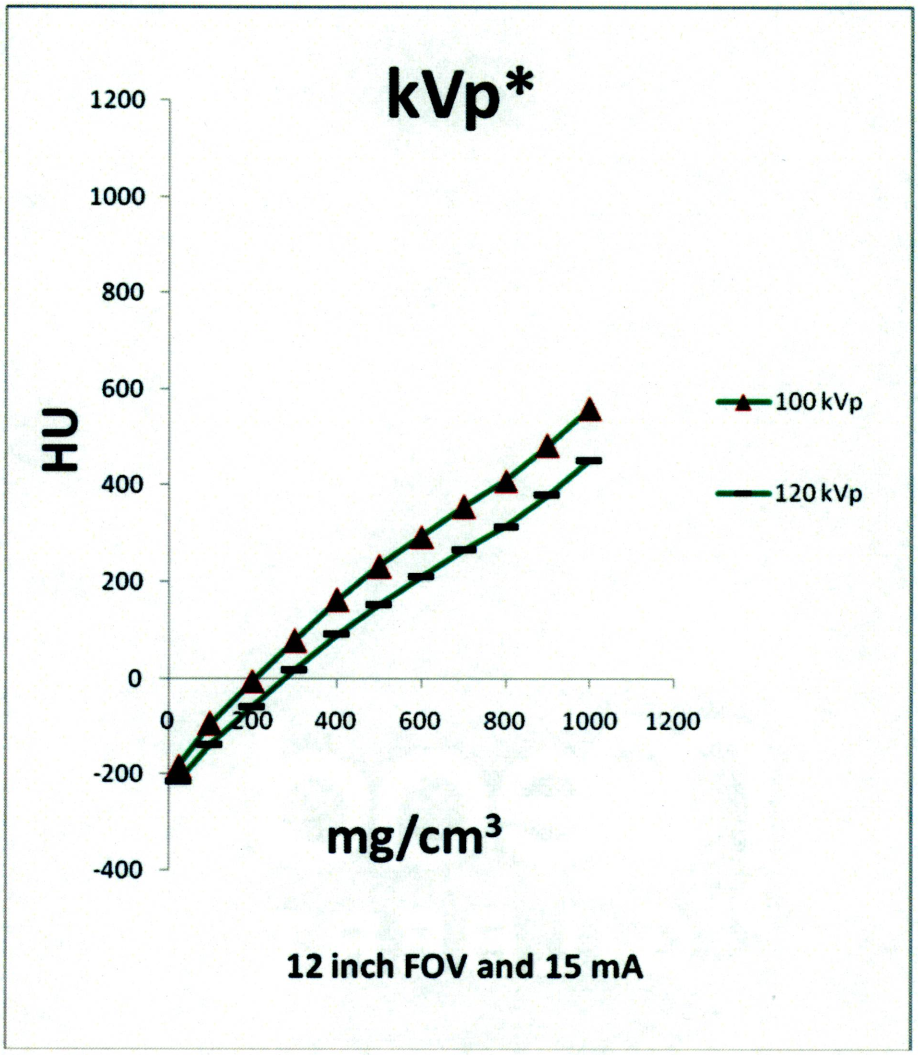

Figure 8. Plotted HU values comparing kVp at the 12 inch FOV and 15 mA.
*ANOVA $p<0.001$

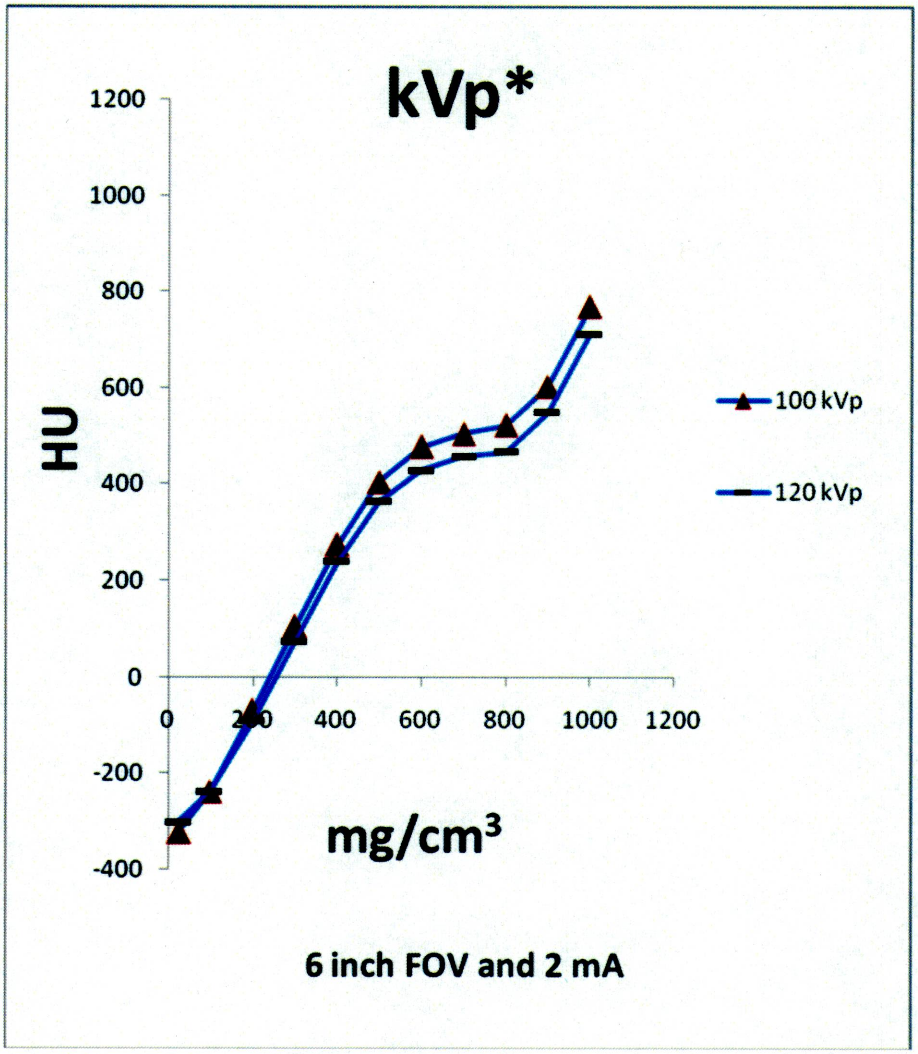

Figure 9. Plotted HU values comparing kVp at the 6 inch FOV and 2 mA.
*ANOVA $p<0.001$

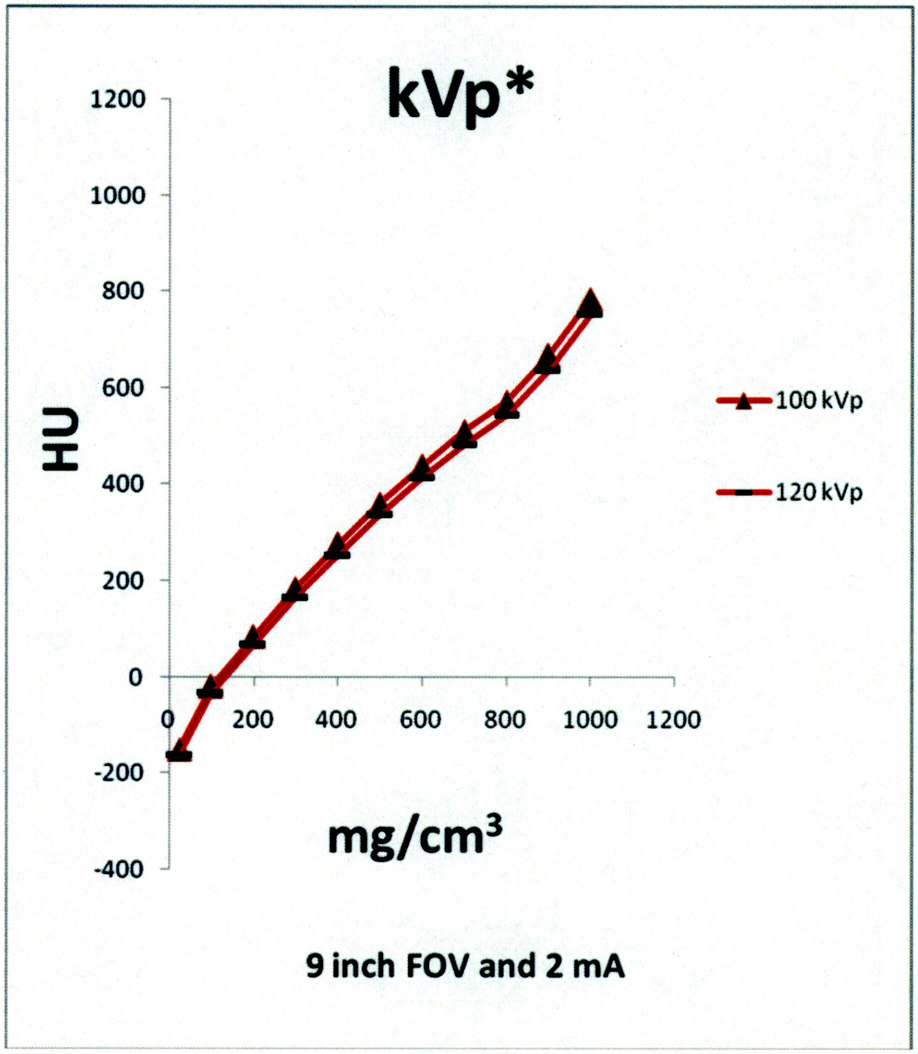

Figure 10. Plotted HU values comparing kVp at the 9 inch FOV and 2 mA.
*ANOVA $p<0.001$

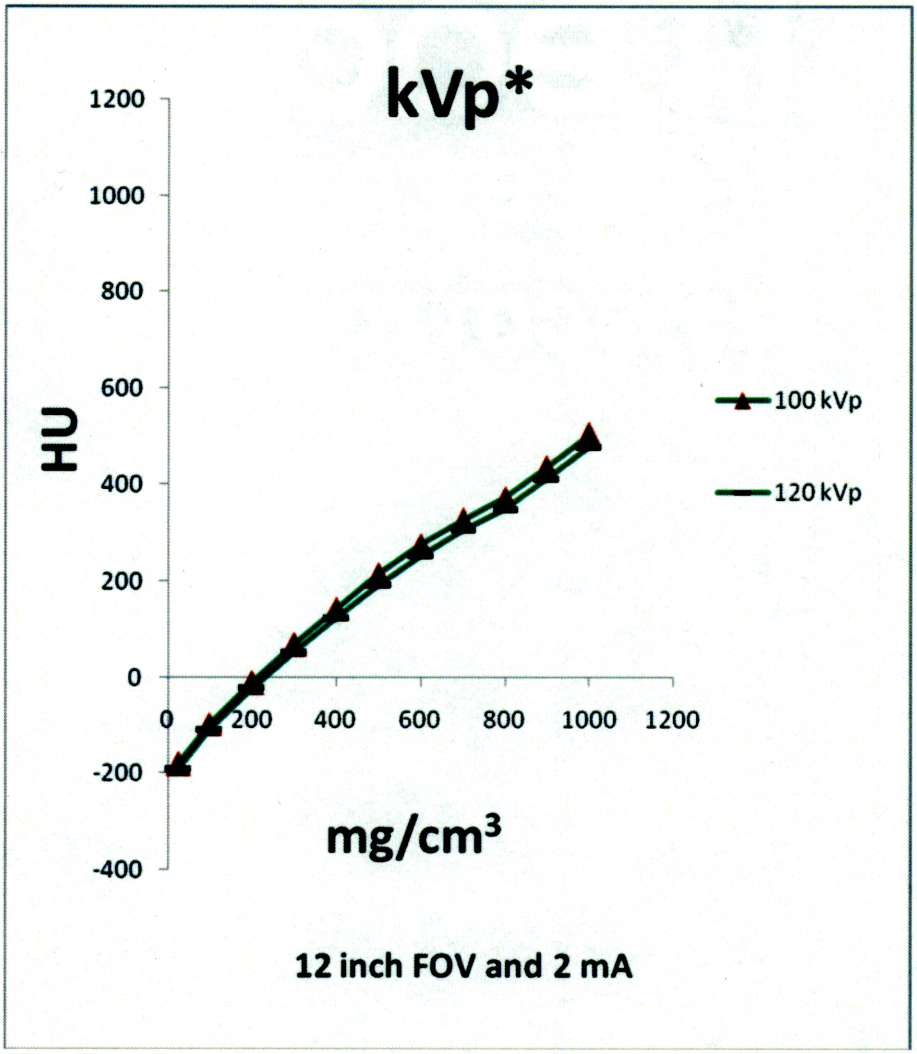

Figure 11. Plotted HU values comparing kVp at the 12 inch FOV and 2 mA.
*ANOVA $p<0.001$

Changing the mA setting from 2 to 15 mA does not significantly change the HU value. Overall, there was less HU difference with varying mA than with kVp, regardless of FOV or kVp settings. (Figures 11-16)

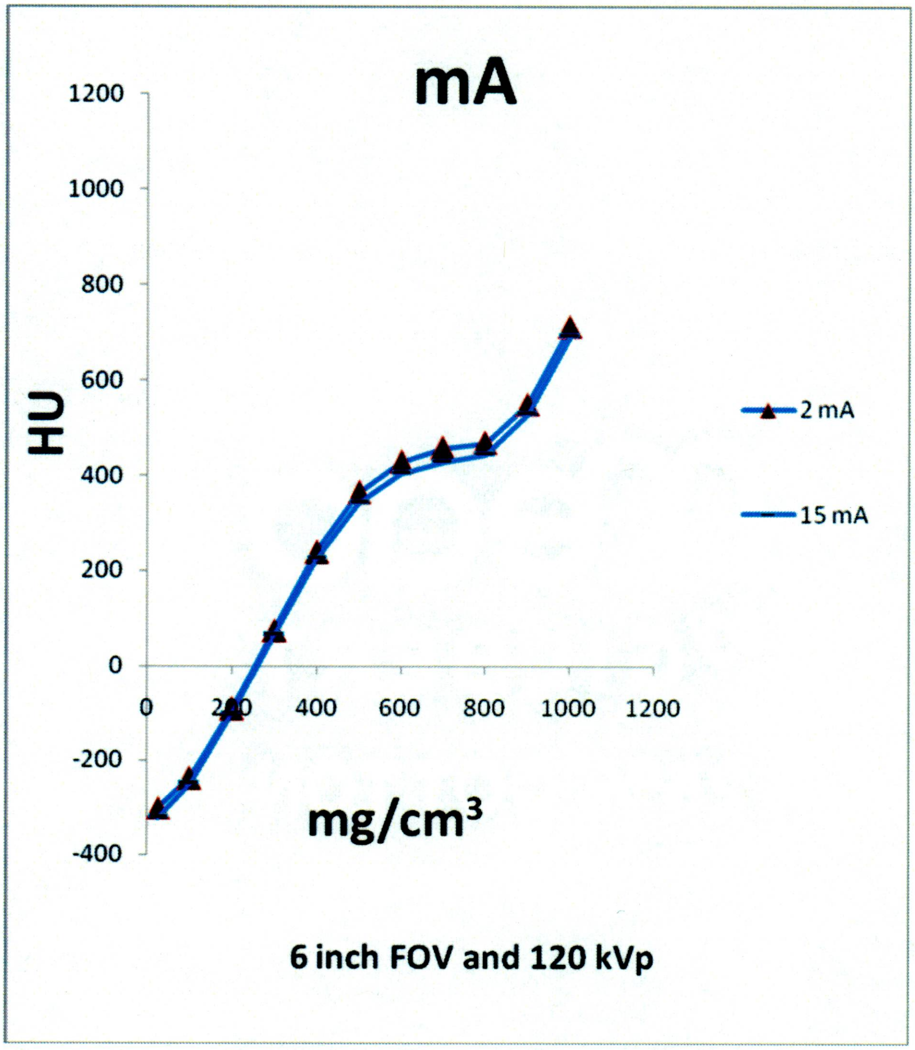

Figure 12. Plotted HU values comparing mA at the 6 inch FOV and 120 kVp.

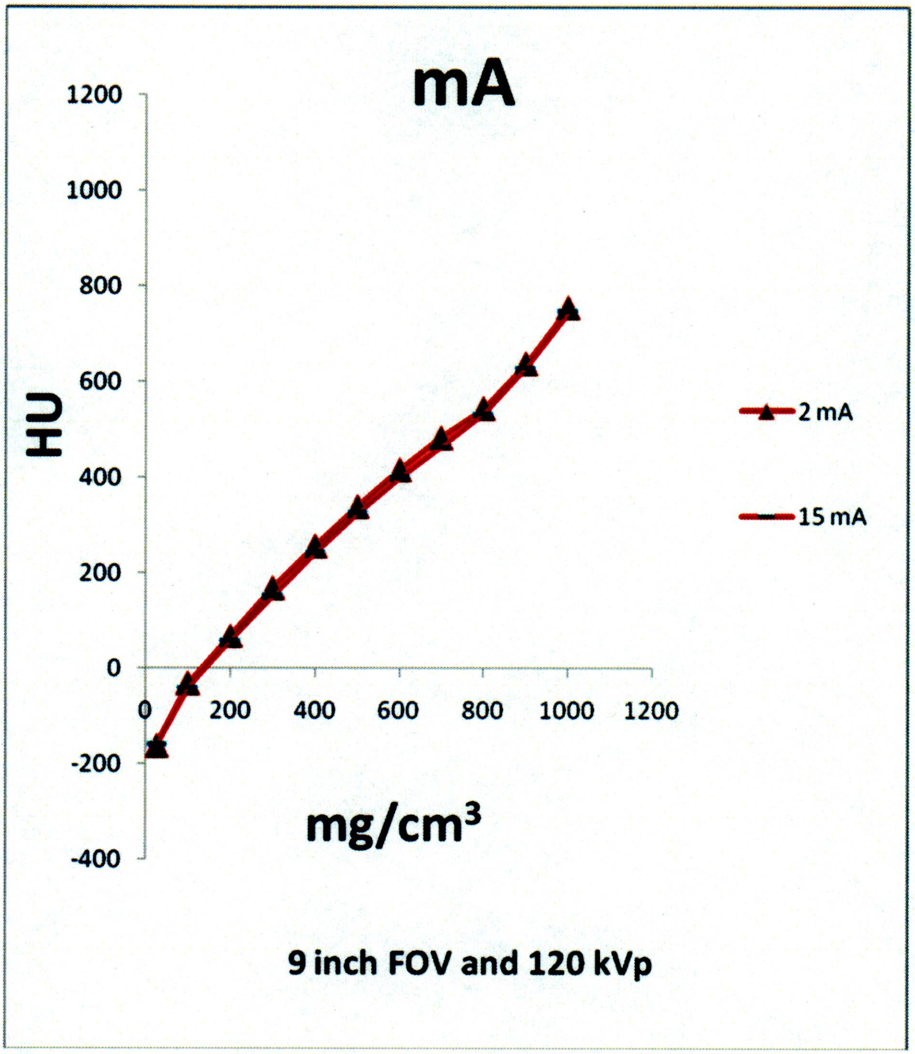

Figure 13. Plotted HU values comparing mA at the 9 inch FOV and 120 kVp.

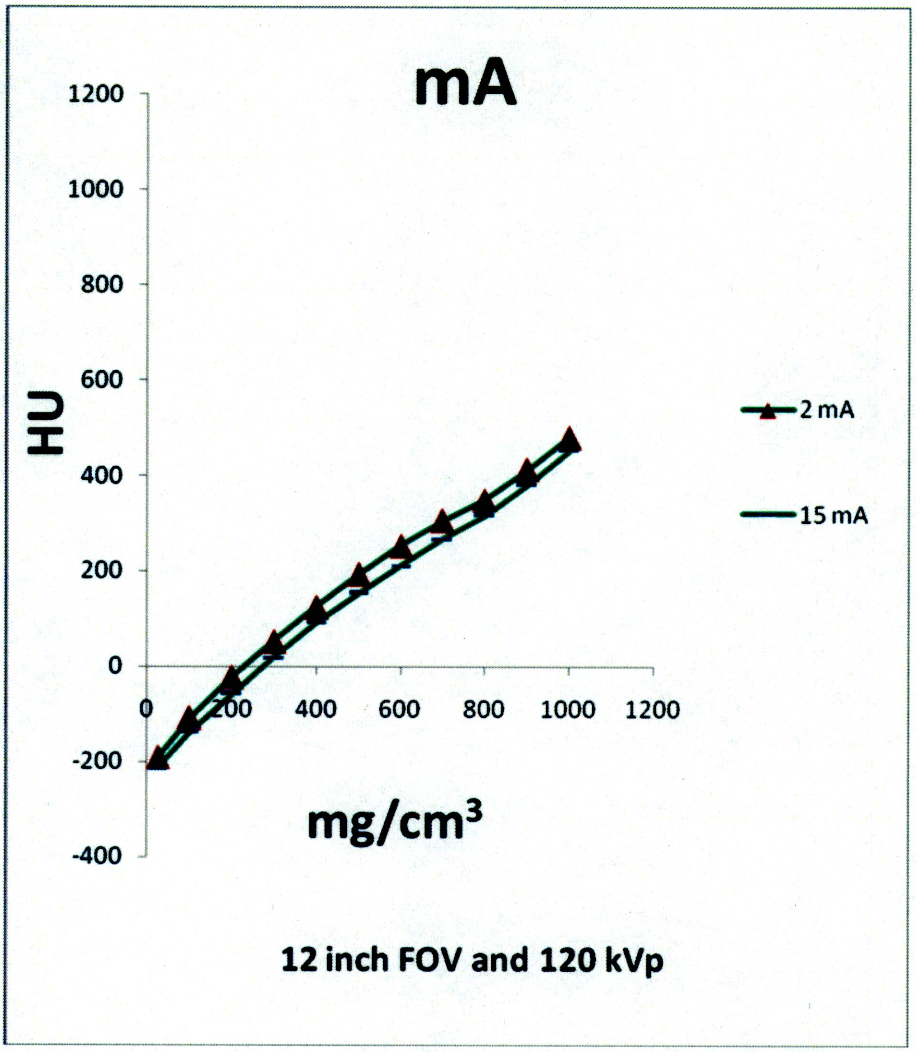

Figure 14. Plotted HU values comparing mA at the 12 inch FOV and 120 kVp.

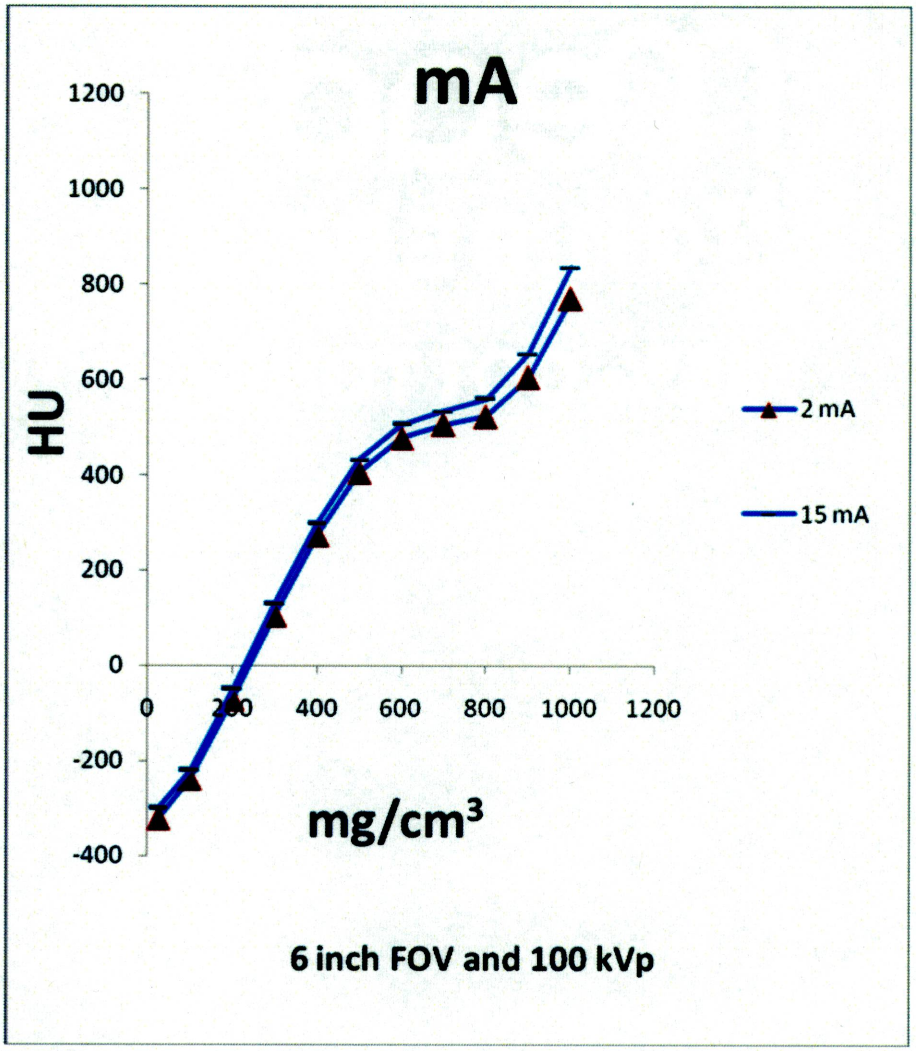

Figure 15. Plotted HU values comparing mA at the 6 inch FOV and 100 kVp.

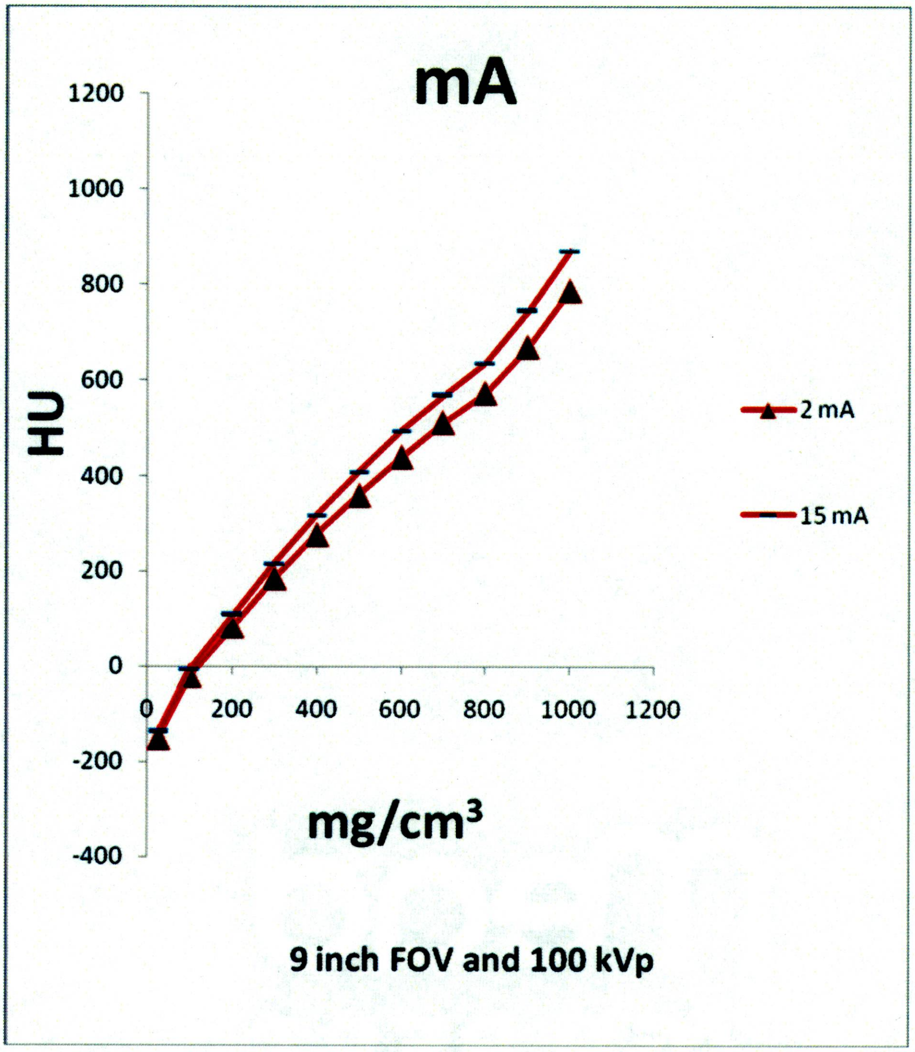

Figure 16. Plotted HU values comparing mA at the 9 inch FOV and 100 kVp.

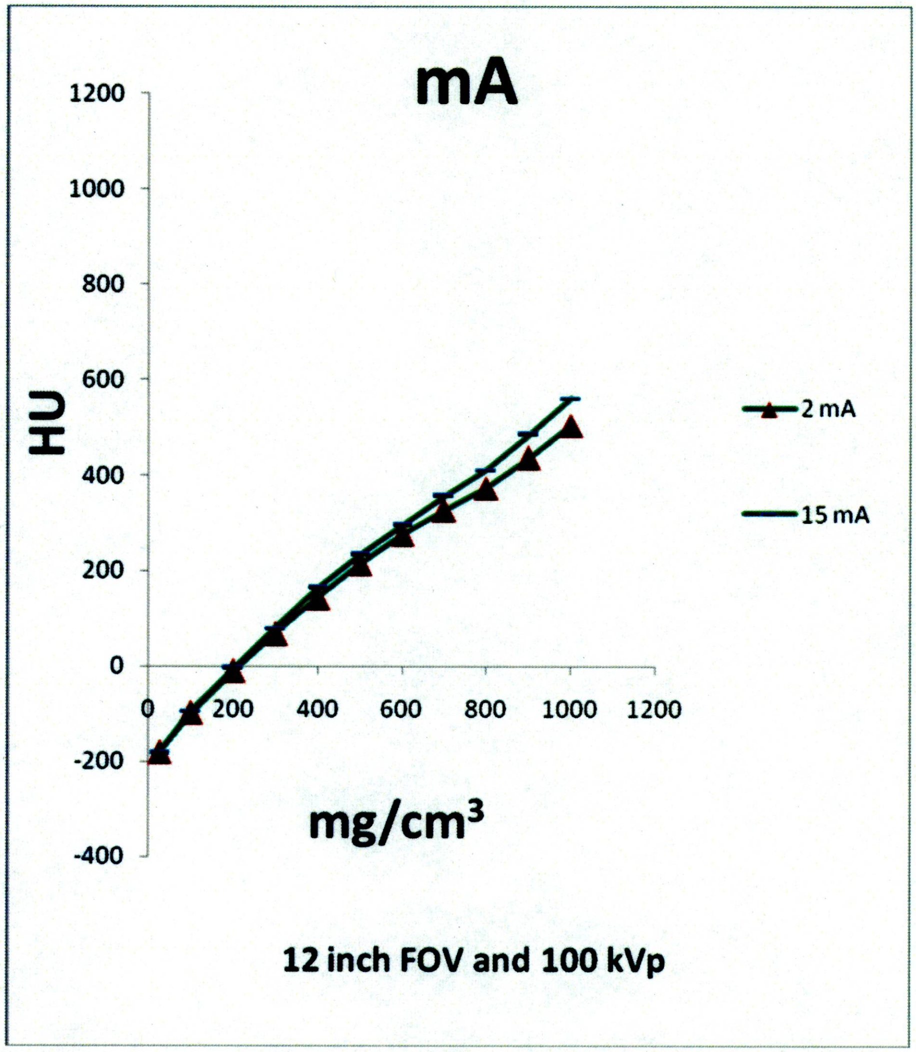

Figure 17. Plotted HU values comparing mA at the 12 inch FOV and 100 kVp.

CHAPER FOUR

DISCUSSION

This study was done to determine the effect of FOV, kVp, and mA, on the HU values of a phantom with a single column of increasing density HA disks. The recorded HU values were consistently of less magnitude than the corresponding HA values. More variation was found in the 6 inch FOV than the 9 and 12 inch. The increased variation with the 6 inch FOV may only be a phenomenon related with this single MercuRay device. The variation found by changing the FOV in this study compares similarly with results obtained with the Newtom 3G. Park found that HU value recorded was statistically different among the three FOV.[24] The same group showed that the ICAT also has a large variation in HU values when the FOV changes from 6 cm, 8 cm, and 13 cm.[26] However there was not a significant difference in HU values when various voxel sizes were compared. This finding supports that the FOV may have more influence on the HU than the voxel size. Another possibility is that there may be a synergistic effect on HU variation when combining the FOV and voxel size.

Increasing the kVp settings from 100 to 120 shows a statistically significant decrease in HU value. This may be explained by the fact that as more energy passes through the phantom a darker image is produced resulting in a lower HU value. Ideally, the software should account for these changes and produce a constant HU value despite the kVp differences.

Araki 2004 described the change in resolution found in the CB MercuRay as image noise. [25] For evaluation of image noise, he used a 16.5 cm cylindrical phantom filled with water. Image noise was expressed as standard deviations of the HU value with all available FOV's in the center of the phantom with the settings of 120 kV, 15 mA, and 10 mA. This study shows a general increase in noise with the smaller FOV and lower kVp settings. If image noise correlates to HU values, his results support the variation we found in HU values with the smaller FOV and lower kVp settings.

With the growing concern of radiation dosage [27, 28], a very significant finding of this study is the minimal amount of variation in the HU seen when changing from 15 mA to 2 mA. This finding will be beneficial in applications when multiple scans of the same patient are necessary. The total radiation dosage can be greatly reduced with the 2 mA setting and the HU values will remain accurate. This finding is supported by a recent study using the 2 mA setting in various diagnostic procedures. [29] That study focused on the clinical applications while evaluating the effects of changing settings on the CB MercuRay. The study used 32 images of a fresh human cadaver heads and 16 images of a dry skull. Clinician's were asked to identify specific anatomy and determine whether it was of diagnostic quality. After evaluation of the images produced by the CB MercuRay, the authors suggested that in order to lower radiation dosages, the 2 mA setting would be clinically sufficient most of the time in the 9 inch and 12 inch FOV.

When adjusting values to 0 baseline, the most accurate results were found with the 9 inch FOV. A calibration device may prove to be useful in creating a baseline correction at 0 HU. Currently, the CB MercuRay is calibrated daily to air and infrequently to both air and water. There may be an advantage to daily calibration to a device similar to the one we have constructed in this experimental design. Until a new calibration system is developed, the 9 inch FOV may provide the most accurate HU values.

CHAPTER FIVE

CONCLUSIONS

1) The results show that there is a statistical difference in HU values with FOV and kVp. However, no significant differences in HU values were found when changing from 2 mA to 15 mA.

2) When repeated scans are indicated, follow up scans can be acquired in 2 mA while maintaining highly comparable HU values.

3) When comparable HU values are desired, it will be prudent to keep the FOV and kVp settings consistent, and use a calibration device.

4) Future comparative studies using different CB MercuRays are needed.

REFERENCES

1. Jaffin RA, Berman CL. The excessive loss of Branemark fixtures in type IV bone: a 5-year analysis. J Periodontol 1991;62:2-4.

2. Ulm C, Kneissel M, Schedle A, Solar P, Matejka M, Schneider B, et al. Characteristic features of trabecular bone in edentulous maxillae. Clin Oral Implants Res 1999;10:459-467.

3. Ulm CW, Kneissel M, Hahn M, Solar P, Matejka M, Donath K. Characteristics of the cancellous bone of edentulous mandibles. Clin Oral Implants Res 1997;8:125-130.

4. Lekholm U ZG. Patient selection and preparation. In: Branemark P-I, Zarb CA & Albrektson T (eds). Tissue-integrated prostheses: Osseointegration in clinical dentistry. . Chicago: Quintessence Publishing 1985:1999-1210.

5. Misch CE. Density of bone: effect on treatment plans, surgical approach, healing, and progressive bone loading. Int J Oral Implantol 1990;6:23-31.

6. Johansson P. Assessment of bone quality from cutting resistance during implant surgery. International Journal of Oral & Maxillofacial Implants 1994;9:279-288.

7. Hounsfield G. Computed Medical Imaging. Science 1980;210:22-28.

8. MR Norton GC. Bone Classification: an objective scale of bone density using the computerized tomography scan. . Clin Oral IMplants Res 2001;12:79-84.

9. Shapurian T, Damoulis PD, Reiser GM, Griffin TJ, Rand WM. Quantitative evaluation of bone density using the Hounsfield index. Int J Oral Maxillofac Implants 2006;21:290-297.

10. Ikumi N, Tsutsumi S. Assessment of correlation between computerized tomography values of the bone and cutting torque values at implant placement: a clinical study. Int J Oral Maxillofac Implants 2005;20:253-260.

11. Stoppie N, Pattijn V, Van Cleynenbreugel T, Wevers M, Vander Sloten J, Ignace N. Structural and radiological parameters for the characterization of jawbone. Clin Oral Implants Res 2006;17:124-133.

12. Todisco M, Trisi P. Bone mineral density and bone histomorphometry are statistically related. Int J Oral Maxillofac Implants 2005;20:898-904.

13. Closmann JJ, Schmidt BL. The use of cone beam computed tomography as an aid in evaluating and treatment planning for mandibular cancer. J Oral Maxillofac Surg 2007;65:766-771.

14. Gracco A, Lombardo L, Cozzani M, Siciliani G. Quantitative evaluation with CBCT of palatal bone thickness in growing patients. Prog Orthod 2006;7:164-174.

15. Guerrero ME, Jacobs R, Loubele M, Schutyser F, Suetens P, van Steenberghe D. State-of-the-art on cone beam CT imaging for preoperative planning of implant placement. Clin Oral Investig 2006;10:1-7.

16. Pohlenz P, Blessmann M, Blake F, Heinrich S, Schmelzle R, Heiland M. Clinical indications and perspectives for intraoperative cone-beam computed tomography in oral and maxillofacial surgery. Oral Surgery, Oral Medicine, Oral Pathology, Oral Radiology, and Endodontology 2007;103:412-417.

17. . Kobayashi K, Shimoda S, Nakagawa Y, Yamamoto A. Accuracy in measurement of distance using limited cone-beam computerized tomography. Int J Oral Maxillofac Implants 2004;19:228-231.

18. Lascala CA, Panella J, Marques MM. Analysis of the accuracy of linear measurements obtained by cone beam computed tomography (CBCT-NewTom). Dentomaxillofac Radiol 2004;33:291-294.

19. Loubele M, Maes F, Schutyser F, Marchal G, Jacobs R, Suetens P. Assessment of bone segmentation quality of cone-beam CT versus multislice spiral CT: a pilot study. Oral Surg Oral Med Oral Pathol Oral Radiol Endod 2006;102:225-234.

20. Marmulla R, Wortche R, Muhling J, Hassfeld S. Geometric accuracy of the NewTom 9000 Cone Beam CT. Dentomaxillofac Radiol 2005;34:28-31.

21. Mischkowski RA, Pulsfort R, Ritter L, Neugebauer J, Brochhagen HG, Keeve E, et al. Geometric accuracy of a newly developed cone-beam device for maxillofacial imaging. Oral Surg Oral Med Oral Pathol Oral Radiol Endod 2007.

22. Aranyarachkul P, Caruso J, Gantes B, Schulz E, Riggs M, Dus I, et al. Bone density assessments of dental implant sites: 2. Quantitative cone-beam computerized tomography. Int J Oral Maxillofac Implants 2005;20:416-424.

23. Lee S, Gantes B, Riggs M, Crigger M. Bone density assessments of dental implant sites: 3. Bone quality evaluation during osteotomy and implant placement. Int J Oral Maxillofac Implants 2007;22:208-212.

24. Park HJ, Kim YJ, Caruso J, Crigger M, Gantes B. Factors influencing contrast resolution of a Cone Beam Computed Tomography. Newtom 3G. Poster Presentation Academy of Osseointegration 2008.

25. Araki K, Maki K, Seki K, Sakamaki K, Harata Y, Sakaino R, et al. Characteristics of a newly developed dentomaxillofacial X-ray cone beam CT scanner (CB MercuRay): system configuration and physical properties. Dentomaxillofac Radiol 2004;33:51-59.

26. Kim YJ, Park HJ, Schulz E, Riggs M, Gantes B, Crigger M. Factors influencing contrast resolution of a cone beam computed tomography. ICAT. Poster Presentation Academy of Osseointegration 2008.

27. Brenner DJ, Hall EJ. Computed tomography--an increasing source of radiation exposure. N Engl J Med 2007;357:2277-2284.

28. Sternberg S. Unneccessary CT scans exposing patients to excessive radiation. USA TODAY, 2007.

29. Kwong JC, Palomo JM, Landers MA, Figueroa A, Hans MG. Image quality produced by different cone-beam computed tomography settings. Am J Orthod Dentofacial Orthop 2008;133:317-327.